Stress Distribution along the Involute Curve of Spur Gears

Namam M. Ahmed

Institute of Technology - Sulamani / Kurdistan, Iraq

Abstract

In this study attempts are carried out to determine the stress distributions along the involute curve of the spur gears. For this purpose photoelastic method and NASTRAN/MSC software are used. The results showed that the maximum applied stress occurs on the top land of teeth, and then that amount is decreased when the applied load positions change toward the bottom land, i.e. during rotation in practical. The results of NASTRAN method showed that the applied stress on the fillet radius is decreased, with lowering the load location from topwards to downwords of gear teeth, and the minimum applied stresses are obtained, between the pitch circle and dedendum circle, in particular at 1.5-1.6 module of the total tooth height equals 2.25 module, and then the applied stresses are increased again. However, in photoelastic method the applied stresses were decreased continuously to the bottom land. The reasons behind such results can be attributed to the type of failure theories, in NASTRAN software, that are used for stress calculation characterization, i.e. considering types of applied stresses, such as bending, direct compressive, and shear stresses. Different standard mathematical equations are used to compare the results between theoretical and practical methods of stress gears. Practical calibration is used to determination the fringe order value of photoelastic materials (PLM-4) used in this study.

Introduction

Essentially, since gears have not a uniform shape, stress determination processes of gears along the entire surface have become important subjects by many investigators, and relevant organizations. In general, designers and manufactures recognized a fillet region

in gears as a highest stress point. In this region, stress concentration factor (K_t) is a main consideration of stress distribution in gears. Therefore, in addition to many theoretical equations, and diagrams, there are several practical methods, such as photoelasticity, strain gauges, have been established for this purpose [1,2]. For instance, over 50 years ago, both Dolan and Broghamer investigated the photoelasticity method for recognizing the stress distribution pattern on spur gears. They determined K_t as a ratio between maximum stress ($\sigma_{max.}$) on the fillet region, and nominal stress ($\sigma_{nom.}$) on other uniform sections. This method still constitutes as a primary source of information on K_t [1-4].

The two previous papers showed complete results regarding the effect of critical geometries, height, (h), and thickness (t), [5], and pressure angle ϕ [6] on K_t of spur gears, using photoelastic method, and NASTRAN software. In this study, the profile of stress change along the involute curve would be shown using a ratio $\sigma / \sigma_{max.}$, where σ is a stress of the fillet radius when load applied locates at any point along the involute profile, and $\sigma_{max.}$ is stress of the fillets radius when the load applied locates at the top land of the gear tooth.

In photoelastic method, a connection between optical and mechanical characteristics is given via the stress optic low [7]:

$$\sigma 1 - \sigma 2 = (N_f * f / b) \qquad 1$$

Where; $\sigma 1$ and $\sigma 2$ are the principal stresses at the point, N_f is a fringe number, b is a thickness of the photoelastic model (mm), and f is the stress optic constant (MPa.mm/fringe). Although N_f is standardized and evaluated in literatures [8-11], and f would be defined by photoelastic material suppliers. Essentially these constants depend on the optical properties of the material and propagated light. In the other mean, the values of photoelastic materials may vary with the batch of resin, temperature, and age. For this reason it is always necessary to calibrate each sheet of photoelastic material at time of the test.

On the other side, in addition to practical methods, there are a lot of equations have been derived to calculate the applied stresses on gears [1]. Such equations mainly used height (h), and thickness (t) of the gears as a two main parameters. However, with changing the approaches of h, and t descriptions, the values of stress also would be changed. In order to show those differences, four different equations are selected in this study.

Experimental Work

Three different groups of spur gears are used in this study, first; $\phi = 20^o$, N = 18; second $\phi = 20^o$, N = 26, third $\phi = 25^o$, N= 18. For each group, four different m; 6, 10, 14, and 20 mm, three different face widths b; 10, 17, 25.4 were prepared. Appendix 1 defines and names each sample for gear teeth selected in this study.

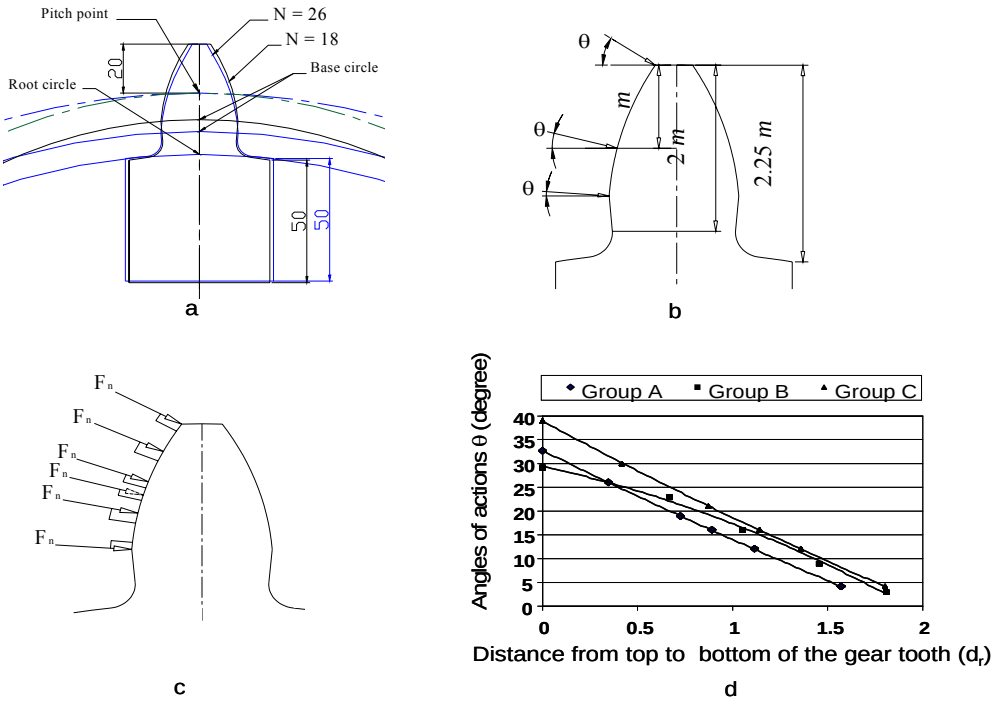

Figure 1; a) involute profile of the spur gear, m=20mm, at different specifications.
b) spur gear depth division according to AGMA.
c) the position of applied loads along the involute cure and their angle of action (θ).
d) the relation between (θ), and applied load position.

Figure 1a shows that the involute profiles change with gear specifications [1,4]. The figure showed that with increasing the number of teeth, the base circle will be larger and less curvatures. Figure 1b shows the total depth of the spur gear tooth, according to AGMA standards, which equals 2.25m, i.e. addendum (a) = module (m), and dedendum (b) = 1.25 m. Figure 1c shows the six positions of load actions along the involute curve. Figure 1d shows the relationship between angle of action, θ, and the radial distance (d_r)

from the top land toward the center of the gear which are indicate as 0.5 m, 1 m, 1.5 m, etc. The figure showed that the maximum (θ) occur at the tip of the gear teeth, and these (θ) are decreased when the load moves along the involute profile toward the fillet radius. Five to six angles of actions are used in this study, which are;

For $\phi = 20^{o}$, N =18; angles of action θ were 32.76, 26, 19, 16, 12, and 4.12˚.

For $\phi = 20^{o}$, N =26; angles of action θ were 29.115, 23, 16, 9, and 2.9799˚.

For $\phi = 25^{o}$, N =18; angles of action θ were 39, 30, 21, 16, 12, and 4.11˚.

For each (θ), four load values Fn, (Fn1 = 29.43, Fn2 = 70.5, Fn3 = 97.88, and Fn4 = 125.26 N, were applied on each tooth. For more details see references [5,6].

To compare the results which were obtained from the practical method (photoelasticity) with numerical method (MSC/NASTRAN), all the gear teeth samples are mentioned above with their specifications (dimensions, load values, load locations are repeated exactly and prepared for MSC/NASTRAN method.

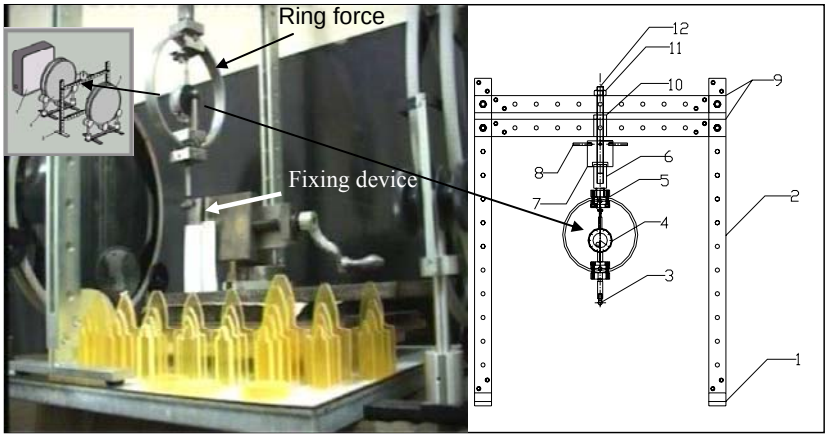

Figure 2 Fixtures and loading device arrangements of photoelastic method.

In order to apply loads on the gear tooth models, as in actual service, it is necessary to design and construct a suitable loading device. In this investigation, certain fixtures were prepared and constructed with loading frame to constraint the samples and apply the load uniformly on gear teeth faces, and the applied load would be normal to the involute profile at any point of contact. The frame consists of several parts, which locates between the polarizer and analyzer of the photoelastic equipment, as shown in Figure 2.

All of the parts are re-constrained by fixing on the thick plate to restrict motions or unbalancing during the load application on the gear tooth. The ring force gauge loading associates with the dial gauge division, and should be calibrated to determine the applied load. Although every ring force manufacturer is supply a calibration certification table. A new calibration for the ring force is carried out to get very accurate results. In order to calculate the net applied load on the gear tooth, the following parameters should be considered [12]:

R_d = Dial gauge reading div, C_m = Mean calibration value N/div, W_e = Weight of the load device N, F_n = Net load N.

$$F_n = (R_d \times C_m) + W_e$$

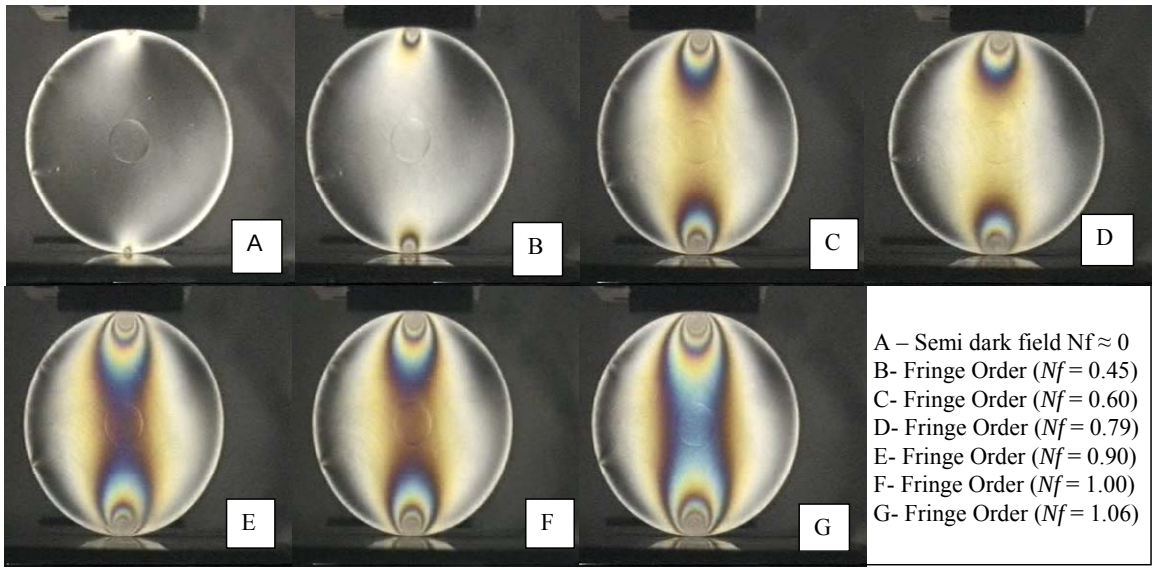

Figure 3 Determination the fringe order values (N_f) using disk method.

The results and calculations showed that the values of mean calibration value (Cm), and weight of load device (We) are equal to 1.369 N/div., and 29.43 N respectively.

On the other side, in order to determine N_f, and f values accurately, a disk with 58.5 mm diameter of the photoelastic material (PLM-4B) is prepared. This material is used by other investigators [13]. The disc model was used for this purpose by other investigators [8-11]. The disk was put on the fixture, with increasing the diametral compressed load values, the fringes are appeared gradually at the center point of the disk as shown in Figure 3. Furthermore, in order to correlate between the applied load and fringe orders ,

the net load values plotted on the y-axis, (using previous calculation for getting the net load), as fringe orders on the x-axis, shown in Figure 4 and, the slope of this graph considered as F_n/N_f , according to the following equation [7-11];

$$f = \frac{8}{\pi D}\frac{F_n}{N_f} \qquad 2$$

The value of F_n/N_f is a slope of curve between F_n and N_f, and equals 234.57 N/fringe. On the other hand, it is obvious that the value of f is independent on the model thickness b.

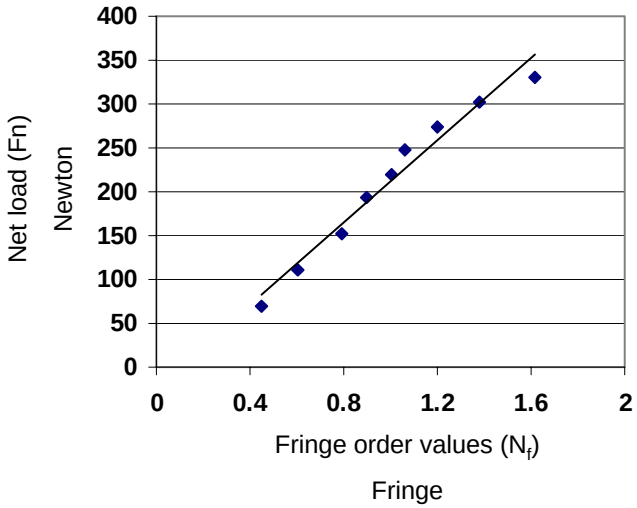

Dial Gauge Reading (R_d) (div.)	Load ($R_d \times C_m$) (N)	Net Load (F_n) (N)	Fringe Order (N_f) (fringe)
30	41.07	69.51	0.45
60	82.14	110.58	0.60
90	123.21	151.65	0.79
120	164.28	192.72	0.90
140	191.66	220.10	1.00
160	219.04	247.48	1.06
180	246.42	274.86	1.20
200	273.8	302.24	1.38
220	301.18	329.62	1.62

Figure 4 The relation between net load and fringe orders to determine the material fringe value, use the values seen in the table in the right side.

The results from equation 2 showed that the average value of (*f*) equals 10.216 N/mm.fringe. Accordingly, after knowing *f*, and the slope Fn/N_f, the values of N_f values can be calculated separately against each applied load. Therefore, with using such calibrated N_f values, Equation 1 can be used directly to calculate the applied stress at any applied load Fn. On the free boundary of the model, either (σ_1) or (σ_2) is equal to zero; hence, the stress tangential to the boundary can be determined directly from the equation [7].

Results

Figure 5 shows the stress distribution, using NASTRAN/MSC software, along the involute curve, for more details see the previous papers [5,6]. The figure showed the highest ratio of (σ/σ_{max}) when the load is applied on the tip of the gear tooth, i.e. (σ/σ_{max}) equals unity. While this ratio decreased with increasing the distance from the top land of the gear tooth to the bottom. Where the height reaches (1.6 modules) the ratio (σ/σ_{max}) approximately equals (0.5). Figures 2b, and 2c show this distribution for (ϕ = 20º, N =26) and (ϕ = 25º, N =18) respectively. Figure 5d shows samples in each group to show the similarity of the variation of (σ/σ_{max}).

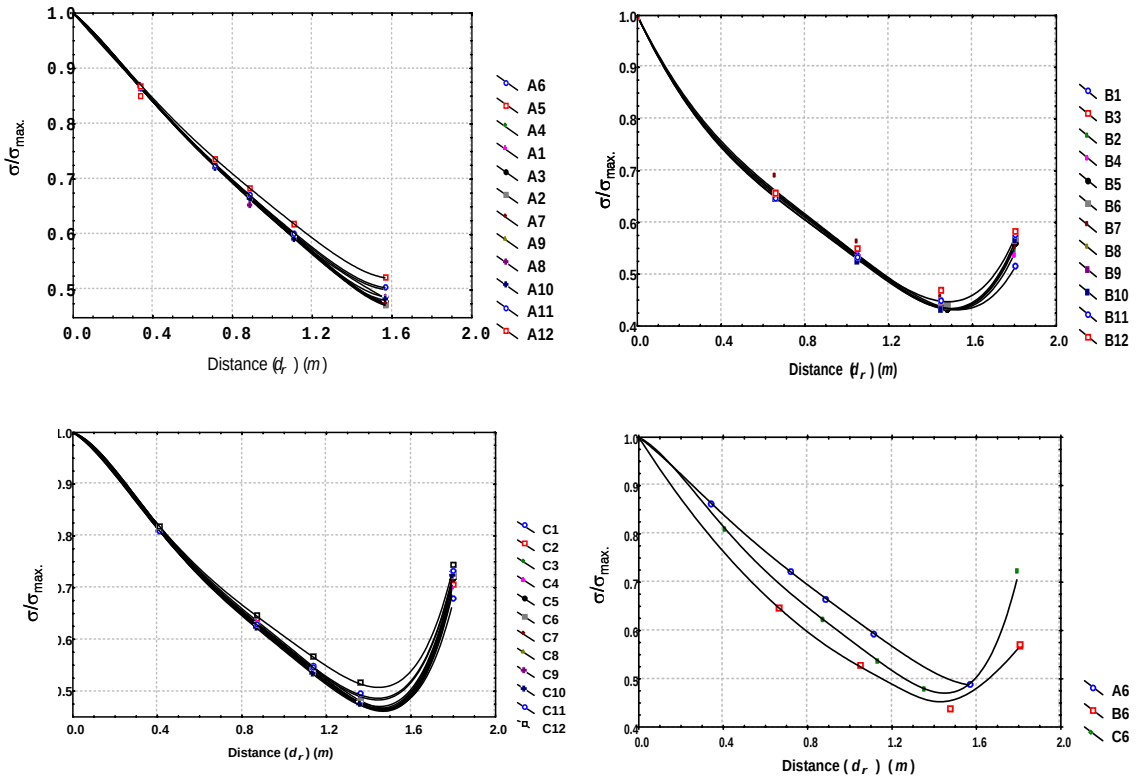

Figure 5 NASTRAN results show the ration (σ/σ_{max}) along the involute curve.

Figure 6 shows the same stress ratio (σ/σ_{max}) with using photoelastic method. Equation 1 is used for calculating the applied stress on the entire involute of gear teeth, by photoelastic method, using Fn, and load values defined in figure 4. The above two figures showed that (similar to the previous condition), the ratio ($\sigma/\sigma_{max.}$) decreased with

decreasing the load applied position with respect to module, until reaches (1.6m) approximately and beyond that the ($\sigma/\sigma_{max.}$) increased again sharply. Since the results of photoelastic results are obtained by practical experiments, due to a limited access of the tools used as fixtures to apply the loads, it was not easy to apply the loads below d_r=1.6m accurately, especially in gears that have had small modules.

This procedure, i.e. stress calculation, had been done by increasing the applied load gradually till the fringes are appeared. The applied stress values were taken for both sides of the gear tooth at fillet radius region (tension and compression) which almost has maximum stress, as shown in Figure 7. The figure showed, in general, that tensile side of the fillet region has higher K_t values than compressive side; see references 4, and 5 for K_t calculations.

As described before, i.e. the ratio ($\sigma/\sigma_{max.}$) is decreased with decreasing the distance between the applied load location and the fillet radius region. This variation is clearer in MSC/NASTRAN than photoelastic method.

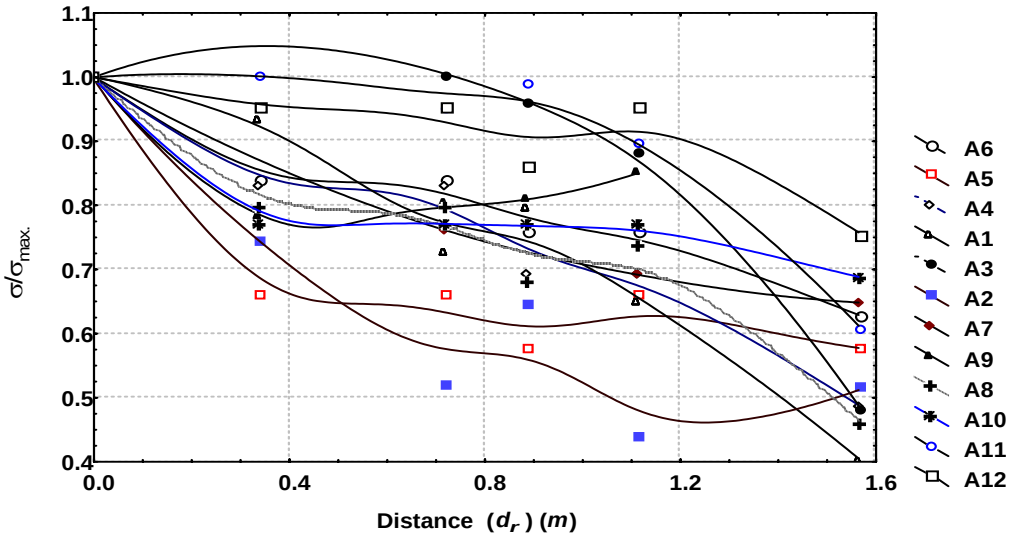

Figure 6 Relation between (σ/σ_{max}) and (d_r) by photoelastic method, for (ϕ = 20º, N = 18) and F_n = 97.88 N

On the other hand, in spite of all failures that occur in gear teeth would be in tension side of the fillet radius by fatigue phenomenon [1-6]. In order to compare the stress values in

both sides, tension and compression, in the fillet radius region, the relations between K_t and module accomplished. Figure 8 shows the variations of K_t values with module. For illustration, samples of $\phi = 20^o$, N = 18, b = 10 mm, and F_n= 29.43 N are selected. The figure showed that the K_t values in tension side are higher than the compression for all modules. This phenomenon remains the same for other applied loads values and other variables like (ϕ, N, b).

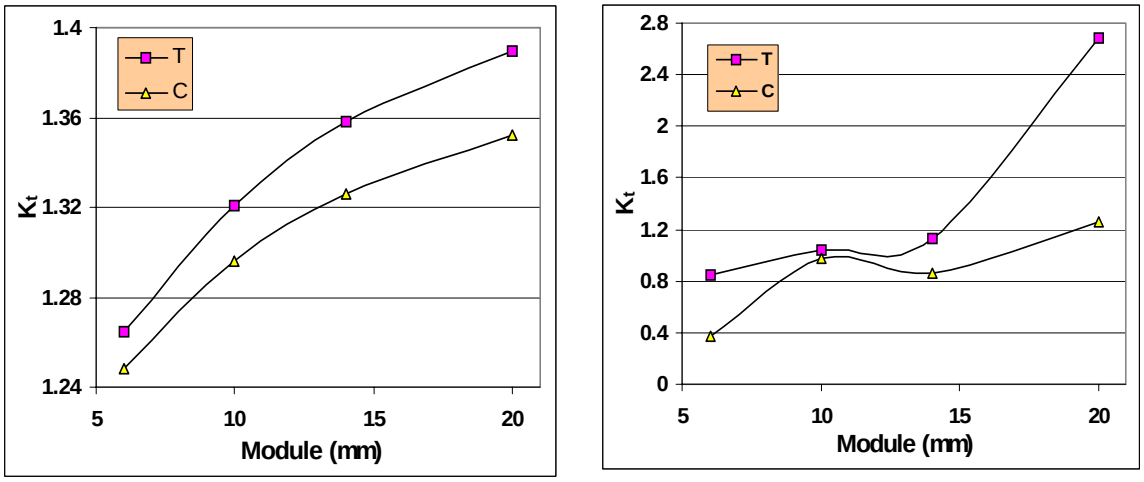

a b

Figure 7 The Kt values in tension and compression values, a) NASTRAN, b) Photoelastic.

In the other side, in order to compare the applied stress values determined by photoelastic, (MSC/NASTRAN) and theoretical equations in the fillet region of the gear samples selected in this study. Four different theoretical equations were selected in addition to both photoelastic and (MSC/NASTRAN) methods. These four theoretical methods are DIN 3990, DIN 3990/E, JGMA and Niemann/GDIN [1,3,4], see Appendix 2.

Figure 8a shows the relation between the applied stress value and module using all theoretical and practical methods selected in this study for ($\phi = 20^o$, $N = 18$, $b = 10$ mm) and ($F_n = 29.43$ N). All the applied stress values that obtained here are determined at fillet region. The figure showed that the applied stress values decreased with increasing the

module. This phenomenon is clear for all methods, while it is more obvious for JGMA method.

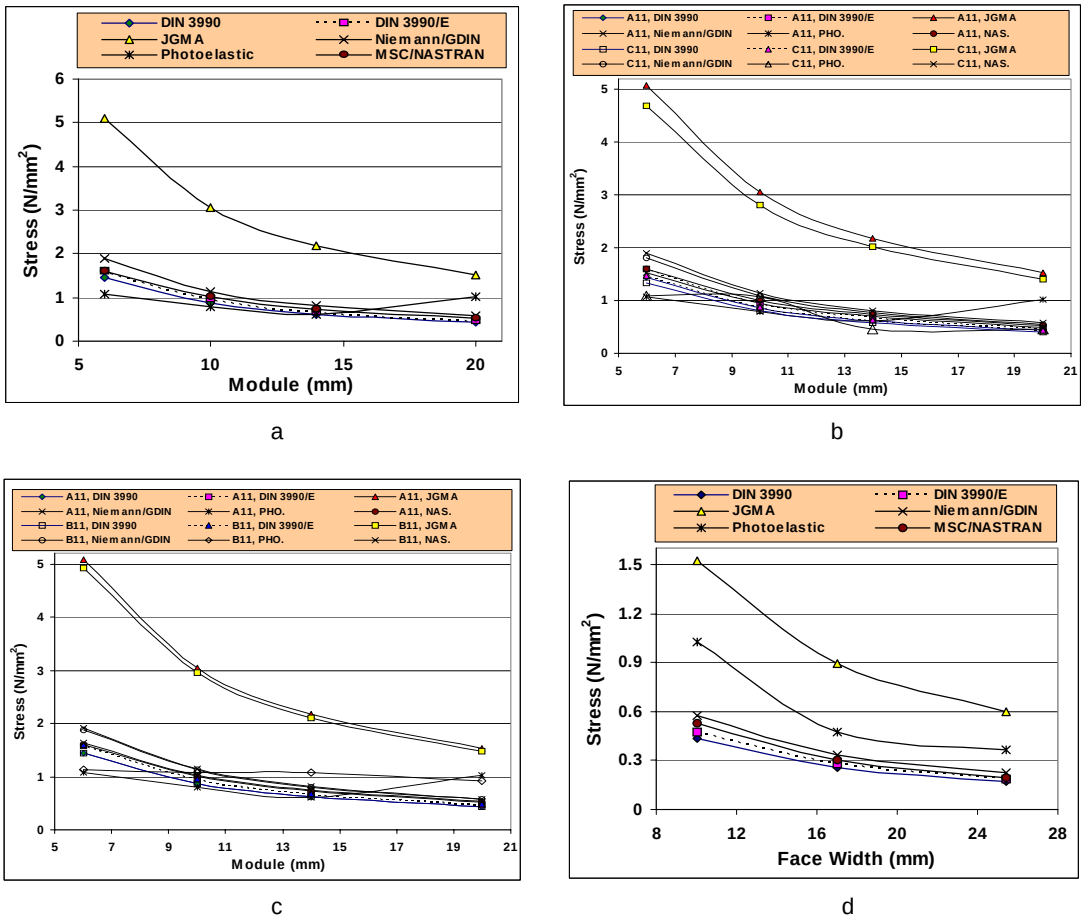

Figure 8 Relation between calculated applied stresses with gears parameters.

a- The relation between stress and face width for A_1 to A_3.
b- The relation between stress and module for A11, and C11 according to ϕ.
c- The relation between stress and module for groups A11, and B11 according to N.
d- The relation between stress and face width for group (A_1 to A_3).

These results can be attributed to the equation formula itself that used for each method. Figure 8b shows the relation between the applied stress and module for two different pressure angles (ϕ = 20º, 25º) with using (N = 18, b= 10 mm, F_n= 29.43 N). The figure shows that with increasing the pressure angles the applied stress decreased and this result coincide with all other approaches. Figure 8c shows the relation between the applied stress and module for different number of teeth. For this purpose two different number of teeth selected which are 18 and 26 with using (ϕ = 20º, b = 10 mm, F_n = 29.43 N). The

figure showed that with increasing the number of teeth the applied stress decreased, and this result coincides with all other approaches. For this purpose in all design calculations, the applied stress usually calculated on the pinion instead of the gear, if both made with the same material. Figure 8d shows that the JGMA has maximum value compared with other methods.

Discussion

Figure 5 showed that the applied stresses are decreased when the load positions are moved from the top land of gear teeth toward the fillet radius. The ratio (σ/σ_{max}) reached 0.5 at (dr) values equal around 1.4-1.6. This result can be explained according to the approaches that had used by Lewis for analyzing the applied loads on the involute profile in gears [1-6]. He described the gear tooth as a cantilever beam, exposed to bending moment. Because the involute profile of gears, i.e. not straight, any applied load is divided in to two main components, tangential force, Ft, (causes bending, and shear stresses), and radial force, Fr, (causes direct compressive stress), as shown in Figure 9. Therefore, very simply the applied bending stress, at fillet radius, can be arranged as below;

$$\sigma = \frac{M\ c}{I} \qquad 3$$

Were, for each cross sectional area, M: is bending moment equals Ft*d,
c: the distance from the neutral axis to the edge layer, and I: moment of inertia.
Although Ft causes small amount of shear stresses over cross sections. At fillet radius positions (A, and B) the shear stresses are zero. Hence, shear stresses can be neglected in such calculations. Therefore, it is obvious that besides compresses stresses, the main applied stress on the fillet radius on gear teeth is the bending stress.
The figure showed that at fillet radius region A, there is a positive (tensile) bending stress (σ_b) , while at fillet radius region B, there is a compressive σ_b. Moreover, due to Fr component, there is a direct compressive stress (σ_c) covering the whole cross section area. Therefore, by summing the two normal stresses ($\sigma_b+\sigma_c$) at each filet region, side A gives low tensile stress value, while side B has a higher compressive stress.

In terms of the variations of (σ/σ_{max}) with (d_r) along the involute profile, were seen in Figures 5, and 6, such results can be attributed to the two immediate opposite variables [1-4]. First, decreasing the applied stress due to decrease the length (d) of the gear tooth, and frequently decrease the bending moment, second, increasing the applied stress due to decreasing θ values. In the other mean, the first variable (decreasing the height-d) has a main influence to reducing the applied bending stress, till the applied load reaches around (1.5m), the ratio (σ/σ_{max}) approximately equals (0.5). However, beyond that point, these effects changed inversely i.e. the second effect (changing reducing θ values) has more effect, i.e. Fn=Ft where θ=0, then the (σ/σ_{max}) increased again after (1.6m).

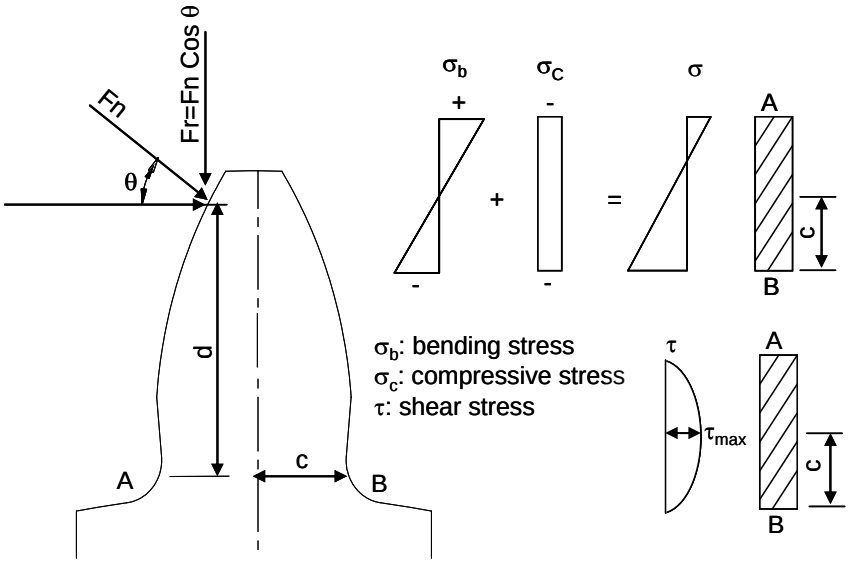

Figure 9 Load and stress analysis on spur gear tooth according to Lewis approach.

In terms of reducing the ratio (σ/σ_{max}), figure 5 showed that the obtained results from NASTRAN method, showed that this ratio is decreased till (d_r =1.6m) and was equal to 0.5. After that height, it increased again. However, the results obtained by photoelastic method showed decreasing continuously. These results can be attributed to the fact that NASTRAN software is software; it is working based on numerical and finite element analysis. Moreover, their calculations also based on one of the common failure theories, such as Von-Mises, Tresca –Guest, etc [4]. Figure 8 proved that each standard formula and equation would give different results of the applied stress on the fillet radius in spur

gears. Therefore, all the results in NASTRAN software depends on the characterization ways of stress calculation, i.e. using each formula of stress calculation, and failure theory might give different results. However, in photoelastic method, the base of calculation is natural behavior of photoelastic material facing applied lights, therefore it is work based on optical analysis.

The results in figures 5-7 showed that the values obtained by (MSC/NASTRAN) were more accurate and realistic. In the other mean, the NASTRAN results showed more linearity and systematic relations with all gear specifications and variables. This phenomenon can be explained in terms of the results obtained by MSC/NASTRAN method which are more accurate than the photoelastic, because in MSC/NASTRAN method the values taken are directly at specified elements, as described before, while in photoelastic method this is more difficult. In addition the values taken from photoelastic method depend strongly on the colors and subsequently depend on the eye precision, skill, etc.

Conclusions

Essentially, the applied stress on the gear profile is decreased from the top land toward the bottom, on the involute curve, until 1.6m approximately, but beyond that stage the applied stress on the fillet radius region increased again. Generally MSC/NASTRAN method gave more uniform results than photoelastic method. Moreover, tension side has higher values of (K_t) than compression side. On the other side, JGMA method has higher values of stress in the fillet region compared with other methods selected.

References

1- Shuting Li “Finite element analyses for contact strength and bending strength of a pair of spur gears with machining errors, assembly errors and tooth modifications” Mechanism and Machine Theory, Vol. 42, (2007) pp. 88-114.

2- Senthilvelan, S., and Gnanamoorthy, R., (2006), “Effect of gear tooth fillet radius on the performance of injection molded Nylon 6/6 gears”, Materials and Design, Vol. 27, pp. 632–639.

3- Pilkey, W.D., (1997), Peterson's Stress Concentration Factors, John Wiley and Sons.
4- Shigley, J. E., (2003), Mechanical Engineering Design, McGraw-Hill.
5- Khoshnaw, F. M., and Ahmed, N. M., (2006), "The determination of the geometric effects of teeth in gear design by using theoretical and practical approaches" Paper presented at 6th International Conference of IDMME, Grenoble, France.
6- Khoshnaw, F. M., and Ahmed, N. M, "The pressure angle effects of spur gears on stress concentration factor"…….
7- Parmjit, S. K., "Automated Photoelasticity", "Research in Automated Photoelasticity", Mechanical and Industrial Engineering, University of Toronto, (1997). pp. 1-4.
8- Anton, R. J., Miskioglu, I., and Subhash, G., "Determination of Residual Stress Fields Beneath a Vickers Indentation Using Photoelasticity", Experimental Mechanics. An International Journal, Vol. 39, No. 3, September, (1999), pp. 227-230.
9- Anton, R. J., Miskioglu, I., and Subhash, G., "Determination of Residual Stress Fields Beneath a Vickers Indentation Using Photoelasticity", Experimental Mechanics. An International Journal, Vol. 39, No. 3, September, (1999), pp. 227-230.
10- J.F. Doyle, J.W. Philips (Eds.), Manual on Experimental Stress Analysis, 5th ed., Society for Experimental Mechanics, Bethel, Connecticut, (1989).
11- Hendry, A. W., "Elements of Experimental Stress Analysis", SI Edition, Pergamon Press Ltd., (1977).
12- Head, K. H., "Manual of Soil Laboratory Testing ", Volume 2: Permeability, Shear Strength and Compressibility Testes, Pentech Press, (1982).
13- Rubayi, N. A., and Tam, H. W. (2006), "Three-dimensional photoelastic study of stresses in rack gears", Experimental Mechanics, Vol. 17, pp. 153-159.

Appendix 1

Group	Label	ϕ (deg)	N	M (mm)	B (mm)
Group A	A_1	20	18	20	10
	A_2	20	18	20	17
	A_3	20	18	20	25.4
	A_4	20	18	14	10
	A_5	20	18	14	17
	A_6	20	18	14	25.4
	A_7	20	18	10	10
	A_8	20	18	10	17
	A_9	20	18	10	25.4
	A_{10}	20	18	6	10
	A_{11}	20	18	6	17
	A_{12}	20	18	6	25.4
Group B	B_1	20	26	20	10
	B_2	20	26	20	17
	B_3	20	26	20	25.4
	B_4	20	26	14	10
	B_5	20	26	14	17
	B_6	20	26	14	25.4
	B_7	20	26	10	10
	B_8	20	26	10	17
	B_9	20	26	10	25.4
	B_{10}	20	26	6	10
	B_{11}	20	26	6	17
	B_{12}	20	26	6	25.4
Group C	C_1	25	18	20	10
	C_2	25	18	20	17
	C_3	25	18	20	25.4
	C_4	25	18	14	10
	C_5	25	18	14	17
	C_6	25	18	14	25.4
	C_7	25	18	10	10
	C_8	25	18	10	17
	C_9	25	18	10	25.4
	C_{10}	25	18	6	10
	C_{11}	25	18	6	17
	C_{12}	25	18	6	25.4

Appendix 2

German Standard DIN 3990

Maximum tooth stress = Tooth root bending stress

$$\sigma_{3990} = \left(\frac{F_n \times Cos\theta}{b}\right)\left(\frac{6 \times h}{t^2}\right)$$

- German Standard DIN 3990/E

$$\sigma = \sigma_{3990} \times \left(1.2 + 0.13 \times \left(\frac{t}{h}\right)\right)^{\left(\frac{1}{1.21+\left(\frac{2.3 \times h}{t}\right)}\right)}$$

This method consists of root bending stress and axial stress experienced at the line of maximum stress in the tooth.

Maximum tooth stress = Tooth root bending stress + tooth axial stress

$$\sigma = \left(\frac{F_n \times Cos\theta}{b}\right)\left(\frac{6 \times h}{t^2}\right) + \left(\frac{F_n \times Sin\theta}{b \times t}\right)$$

- JGMA Standard 401-01

This method consists of root bending stress multiplied by a stress concentration factor.

Maximum tooth stress = Tooth root bending $\times$ stress concentration factor

$$\sigma = \left(\frac{F_n Cos\theta}{b}\right)\left(\frac{6 \times h}{t^2}\right) \times \left(\frac{Cos\theta}{Cos\theta_i}\right)\left[\frac{6 \times \left(\frac{h}{m}\right)}{\left(\frac{t}{m}\right)^2}\right]$$

- Niemann Method

This method consists of bending, axial and shear stress experienced at the line of maximum stress in the tooth root.

Maximum tooth stress = Tooth root bending stress + tooth axial stress + tooth shear stress

$$\sigma = \left(\frac{F_n \times Cos\theta}{b}\right)\left(\frac{6 \times h}{t^2}\right) + \left(\frac{F_n \times Sin\theta}{b \times t}\right) + \left(\frac{F_n \times Cos\theta}{b \times t}\right)$$